Design of Inhibitors of the MurF Enzyme of *Streptococcus pneumoniae* Using Docking, 3D-QSAR, and de Novo Design

Santosh A. Khedkar, Alpeshkumar K. Malde, and Evans C. Coutinho*

Department of Pharmaceutical Chemistry, Bombay College of Pharmacy, Kalina, Santacruz (E),
Mumbai 400 098, India

The biosynthetic pathway for formation of the bacterial cell wall (peptidoglycan) presents an attractive target for intervention. This is exploited by many of the clinically useful antibiotics, which inhibit enzymes involved in the later stages of peptidoglycan synthesis. MurF is one of the four amide bond-forming enzymes (D-alanyl−D-alanine ligating enzyme) that catalyzes the ATP-dependent formation of UDP-MurNAc-tripeptide. In the present study, several MurF inhibitors were docked into the active site of MurF to explore their binding modes and also to gain an insight into the crucial ligand−receptor interactions at the molecular level. The final selection of the "bioactive" conformation of every ligand was influenced by consensus scoring in which various independent scoring functions such as GoldScore, ChemScore, HINT score and X-CScore were employed. Subsequently, 3D-QSAR studies using comparative molecular field analysis (CoMFA) and the new approach comparative residue interaction analysis (CoRIA) have been carried out on the enzyme−inhibitor complexes obtained by docking and postscoring analysis. Finally, new inhibitors have been designed using the de novo approach of Ludi, and the activities of the most promising hits have been predicted with the CoMFA and CoRIA models.

INTRODUCTION

The emergence of multidrug-resistant bacteria has led to an increased demand for new types of antibiotics.[1] The biosynthetic pathway for formation of the bacterial cell wall (peptidoglycan) presents an attractive target for inhibition which is exploited by many of the clinically useful antibiotics (such as penicillin and vancomycin). These antibiotics inhibit enzymes involved in the later stages of the murein biosynthesis pathway.[2] A set of ligases (MurC−F) is responsible for the synthesis of UDP-MurNAc-pentapeptide, a precursor to peptidoglycan biosynthesis common in gram-negative bacteria.[3] In addition, the Mur enzymes are highly conserved among various bacterial species, and therefore, an inhibitor of the Mur enzymes will possess a broad spectrum of activity.[4] Such chemotherapeutic agents may have lesser potential of developing resistance through mutations in a single target protein.
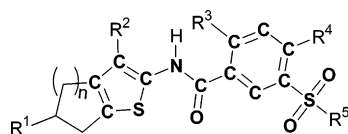
MurF is one of the four amide bond-forming enzymes involved in the synthesis of UDP-MurNAc-pentapeptide. It is a D-alanyl−D-alanine ligating enzyme that catalyzes the ATP-dependent formation of UDP-MurNAc-tripeptide.[5] Over the years aminoalkylphosphinates have been synthesized as transition-state analogs[6] which act as reversible competitive inhibitors of the MurF enzyme of *Escherichia coli*. Recently, the research group at Abbott pharmaceuticals reported analogs of two MurF inhibitors (molecules **1** and **2** in Table 1) discovered via an affinity selection screening technology.[7] The X-ray structures of MurF from *Streptococcus pneumoniae* bound to the leads **1** and **2** (PDB codes 2AM1 and 2AM2, respectively)[8,9] have been solved at 2.5 and 2.8 Å

resolutions, respectively. We have used the technique of docking to explore the binding modes of the structurally different analogs of leads **1** and **2** in the active site of MurF to gain an insight into the crucial ligand−receptor interactions at the molecular level. Subsequently, 3D-QSAR studies using comparative molecular field analysis (CoMFA)[10] and comparative residue interaction analysis (CoRIA)[11] have been carried out on the enzyme−inhibitor complexes obtained by docking and postscoring (i.e., consensus scoring) strategies. Finally, some new inhibitors have been designed using the de novo approach of Ludi, and the activities of the most promising hits have been predicted with the CoMFA and CoRIA models.

COMPUTATIONAL METHODS

Protein and Ligand Preparation. The X-ray structure of *S. pneumoniae* MurF (PDB code 2AM1) has been used as the structure base for modeling of the inhibitors. The ligand and water entries (which are not reported to be crucial for ligand binding) were deleted. Selenomethionine (MSE) and the related HETATM entries in the PDB file were replaced with MET (methionine) and ATM. The hydrogens to all heavy atoms were added with the Biopolymer module of Sybyl (version 7.1, Tripos Inc., U.S.), running under the Linux RedHat Enterprise WS (version 2.1) OS. Sybyl atom and bond types were assigned, and the positions of hydrogens were optimized with 500 iterations each of steepest descents and conjugate gradients using the Tripos force field and Gasteiger−Hückel atomic charges. The structures of the MurF inhibitors were "sketched" in Sybyl, and the energy was optimized to a gradient of 0.001 kcal/mol/Å with the MMFF94 force field[12] and the MMFF94 partial atomic charges. The biological activity data (reported as IC$_{50}$ in

* To whom correspondence should be addressed. E-mail: evans@
bcpindia.org. Phone: +91-22-26670905. Fax: +91-22-26670816.

Table 1. Structures of Inhibitors with Their Experimental Inhibitory Activities (pIC$_{50}$) against *S. pneumoniae* MurF Enzyme

ID	R^1	R^2	R^3	R^4	R^5	n	pIC$_{50}$ (molar)
1	H	CN	Cl	H	—N͡O (morpholine)	2	6.00
2	H	CN	Cl	H	-NEt$_2$	1	5.10
3	H	CN	Cl	H	—N͡O (morpholine)	1	5.05
4	H	CN	Cl	H	-NHMe	1	4.82
5	H	CN	Cl	H	-NHPh	1	4.59
6	H	CN	Cl	H	-NH(CH$_2$)$_3$OH	1	5.10
7	H	CN	Cl	F	—N͡O (morpholine)	1	5.19
8	H	CN	Cl	Cl	-NEt$_2$	1	5.28
9	H	CN	Cl	Cl	—N͡O (morpholine)	1	6.52
10	H	CN	Cl	-NHMe	—N͡O (morpholine)	1	4.21
11	H	-CONH$_2$	Cl	H	-NEt$_2$	1	4.18
12	H	CN	-NH(CH$_2$)$_3$NMe$_2$	H	—N͡O (morpholine)	1	4.13
13	H	CN	Br	H	—N͡O (morpholine)	1	5.38
14	H	CN	Cl	H	-NEt$_2$	2	5.85
15	H	CN	Cl	H	—N͡O (morpholine)	2	5.77
16	Ph	CN	Cl	Cl	—N͡O	2	7.15
17	—⬡—OH	CN	Cl	H	-NEt$_2$	2	7.27
18	-CO$_2$Et	CN	Cl	H	-NEt$_2$	2	5.22
19	—⬡—OH	CN	Cl	Cl	-NEt$_2$	2	7.17
20	—⬡—OH	CN	Cl	Cl	—N͡O (morpholine)	2	7.66
21	H	CN	Cl	H	-NEt$_2$	3	5.47
22	H	CN	Cl	H	—N͡O (morpholine)	3	5.38

micromolar)[7] for these inhibitors was converted to the negative log (base 10) of the IC$_{50}$ value (pIC$_{50}$) on the molar scale (Table 1).

Docking and PostScoring Analysis. The inhibitors were docked into the MurF active site with the program GOLD[13] (version 3.0.1; Cambridge Crystallographic Data Center, U.K.) running under the Windows environment. With any docking program, it is first necessary to determine its effectiveness for the protein under study. The GOLD docking parameters were optimized to reproduce the X-ray pose of molecule **1**. The docking parameters used were as follows: The active site was composed of residues within a 10 Å radius from the centroid of the benzene ring of molecule **1**.

The ligand flexibility options such as flipping of ring corners, amide bonds, and pyramidal nitrogen were switched off, the internal energy offset parameter was switched on (this parameter does not influence the ranking of the ligand poses, but this correction has been reported to improve the correlation between score and affinity).[14] The torsion angle distributions were used from the CSD database. A docking protocol with 20 GA cycles and with the above-mentioned GA settings was run with GoldScore[13,14] as the fitness function. The top five poses ranked by GoldScore for every ligand were archived for postscoring analysis in which rescoring of these conformations was carried out using GoldScore,[13,14] ChemScore,[15] HINT Score[16] and X-CScore[17]

INHIBITORS OF MURF ENZYME

J. Chem. Inf. Model., Vol. 47, No. 5, 2007 **1841**

to find the consensus between different independently developed scoring functions. Rescoring using GoldScore and ChemScore was achieved with the "Rescore" option in which local optimization (simplexing) was used with the GA parameter turned off.

Postscoring with HINT was also carried out with the Sybyl HINT program after modification of the atom names of the terminal residues in the protein as described in the Sybyl HINT manual. The HINT score is a sum of hydropathy interactions between all atom pairs and encodes significant thermodynamic and interaction information in addition to the effect of solvent. The HINT scoring function is reported to be a good indicator of biological activity.[16] The "calculate" and "dictionary" methods as implemented in Sybyl HINT were employed for partitioning the ligand and the protein, respectively. The enzyme area within 10 Å from the respective ligand pose was considered for calculation of the intermolecular hydropathy interaction (HINT) score using the polar and hydrophobic functions separately. X-CScore[17] is an empirical scoring function developed to estimate the binding affinity of a given protein−ligand complex. The terms included in X-CScore include van der Waals interaction, hydrogen bonding, deformation penalty, and hydrophobic effect. The X-CScore is a consensus score of three different scores such as HP-, HM-, and HS-, which differ in the manner of computation of the hydrophobic effect term: the HM-score is calculated with the hydrophobic matching algorithm adopted by SCORE,[18] the HS-score is calculated with the hydrophobic surface algorithm adopted by Bohm's scoring function,[19] and the HP-score is calculated with the hydrophobic contact algorithm.[17] The postscoring using X-CScore (running on a SGI Fuel machine with Irix6.3 OS) was performed with all the three scores, HP-, HM- and HS-Scores.

3D-QSAR Analyses. The dataset was divided into training (18 molecules) and test (4 molecules) sets for use in the QSAR studies. A comparative molecular field analysis (CoMFA)[10] study was carried out with the Sybyl QSAR module. The most crucial input for CoMFA is the alignment of the molecules. Three alignments were used to develop the CoMFA models to capture the spatial flexibility of the ligands: *receptor-based* (using the receptor-bound conformations), *atom-fit*, and *field-fit* alignments. For receptor-based alignment (Figure 3A), the pose of each ligand echoed consensually as being the best pose by GoldScore, HINT Score, and X-CScore (consensus) was used; this was also taken to be the most probable bioactive conformation. An alignment of ligands was achieved by reading in the "best" docked pose with reference to the receptor protein followed by deletion of the receptor coordinates. For atom-fit alignment (Figure 3B), the heavy atoms in the common substructure (indicated by bold characters in the structure in Table 1) were used. The CoMFA fields (steric and electrostatic) for each ligand were calculated and used for alignment in the field-fit alignment (Figure 3C). The CoMFA steric and electrostatic interactions at each grid point (spacing 2.0 Å) was calculated with a sp^3 carbon atom having +1.0 charge as the probe and the standard Tripos forcefield. A distance-dependent dielectric constant of 1.0r was used in the calculation of the electrostatics. The steric field was truncated at points where the value exceeded 30.0 kcal/mol, and the
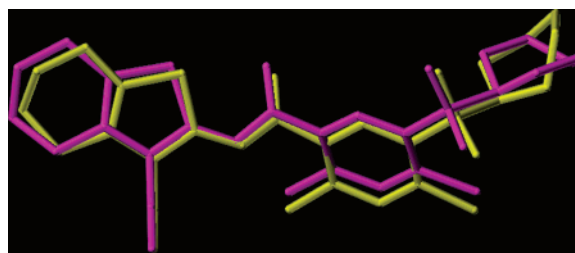

Figure 1. Superimposition of the X-ray pose (magenta) and the pose obtained through docking with the program GOLD (yellow) for molecule **1,** thus validating the docking protocol.

electrostatic fields were ignored at those lattice points where the steric interactions were high.

The recently reported new QSAR approach, termed comparative residue interaction analysis (CoRIA),[11] was employed to extract the crucial ligand−receptor interactions essential to activity. It is an adaptation of the QSAR formalism in a receptor setting to answer both the type (qualitative) and the extent (quantitative) of ligand−receptor binding, through the use of descriptors that account for the thermodynamics of ligand−receptor binding. It can be used to identify crucial interactions of inhibitors with the enzyme at the residue level, which can be gainfully exploited in optimization of the inhibitory activity of the ligands. As a first step, the selected ligand−receptor complexes were minimized for optimization of hydrogen positions, keeping all heavy atoms fixed. The Coulombic and van der Waals interaction energies of each ligand with active site residues (10 Å from the centroid of the benzene ring in molecule **1**, Table 1, and Figure 1) were calculated with the CFF91 force field in the Discover3 module of Insight II (Accelrys Inc., U.S.). The strain energy of every ligand was calculated as the difference between the energy of the ligand bound to the receptor and the energy of the ligand in vacuo. The energy minimization of the ligand in vacuum was carried out to a gradient of 0.001 kcal/mol/Å with the Discover3 module. The solvation free energy for receptor bound conformation of every ligand was calculated using the program Quasar.[20] The nonbond interaction energies and other thermodynamic descriptors form the X-variables (descriptors) in the QSAR analysis, which are correlated to the biological activity (Y-variable) using G/PLS statistics[21] to derive the CoRIA models. The number of PLS components, GA runs and terms in the equation were set as 3, 20 000, and 4, respectively. The top ten equations were analyzed for the frequency of occurrence of X-variables.

De Novo Ligand Design. A de novo design of inhibitors was undertaken with the program Ludi (Insight II, Accelrys Inc, U.S.) through the "Energy Estimate" scoring functions[19] for evaluation of the quality of new ligands. These scoring functions estimate the change in free energy upon binding of the fragment to the receptor, and the scores correlate with the inhibition constant K_i. Each fragment is evaluated as a function of the potential number of hydrogen bonds, hydrophobic and ionic contacts, and a penalty for freezing of the internal degrees of freedom. The active site of the MurF enzyme comprising residues within a 10 Å radius from the centroid of the benzene ring in molecule **1** was considered for design of inhibitors by the Ludi program, which was run in the "standard mode" and with the Ludi CAP2002 library (presently comprising approximately 78 000 fragments). A

conformational search of the fragments was done with consideration of two rotatable bonds simultaneously. The remaining parameters were used at their default settings.

RESULTS AND DISCUSSION

The peptidoglycan biosynthetic pathway has long been described as a suitable ground for the development of antibiotics. In this regard, the four ligases (MurC, D, E, and F) have been shown to bear significant blocks of homology.[22] These reflect elements of shared macromolecular structure necessary for substrate recognition or catalytic function, or both. X-ray crystallography studies reveal that the 3D structure of these enzymes consists of three open "α/β-domains".[23] The ligand binds in the substrate-binding region (located at the interface of the three domains) and induces closure of the domain. This arrangement of domains represents a large conformational change for the C-terminal domain relative to its corresponding position observed in the apo structure of the enzyme. A compact topology of the cocrystal structures (PDB codes 2AM1 and 2AM2) suggests that the protein has been captured in a "closed" state. The compounds possibly induce or stabilize the closed conformation, as it was observed that the protein failed to crystallize in the apo form but readily crystallized in the presence of a ligand. This compact conformation of the protein in the cocrystals is apparently dependent upon ligand binding.[9]

Docking and PostScoring (Consensus Scoring) Analysis. The GOLD program was used to find the best pose for every ligand in the binding site of the MurF enzyme. Docking with the program GOLD could successfully reproduce the X-ray pose of ligand **1** with an rmsd of 0.5 Å (heavy atoms, Figure 1). An unusal boat conformation of the morpholine ring of ligand **1** is observed in the X-ray structure (PDB code 2AM1). To reproduce the X-ray conformation of the morpholine ring, it was necessary to build the morpholine ring in a boat conformation and to "switch off" the option for ligand flexibility—flip ring corners in the docking protocol.

To deal with the deficiencies of the currently available scoring functions, one can either identify a good score for the "target" protein or use a consensus score to rank protein—ligand complexes according to their binding affinities.[24] The best pose for every ligand predicted using GoldScore was rescored with three different scorings: ChemScore, HINT Score, and X-CScore. A correlation analysis of the experimental binding affinities of the inhibitors with GoldScore reveals a Pearson R value of 0.55, whereas ChemScore shows no significant correlation. The HINT score shows a significant correlation with the inhibitory activities of ligands, with a Pearson R value of 0.92. The polar and hydrophobic components of HINT score bear Pearson R values of 0.75 and 0.65, respectively. X-CScore shows a Pearson R value of 0.78, whereas for HP-Score, HM-Score and HS-Score, the Pearson R values are 0.75, 0.70, 0.75, respectively. A Pearson R value of 0.70 for log P (calculated using X-CScore) is obtained. Finally, a consensus score was established by amalgamation of GoldScore, HINT score, and X-CScore (and their components). The best combination of scoring functions to formulate a consensus score was achieved by combination of HINT score and X-CScore, which showed a Pearson R value of 0.71. Although there was a marginal improvement over the individual representa-
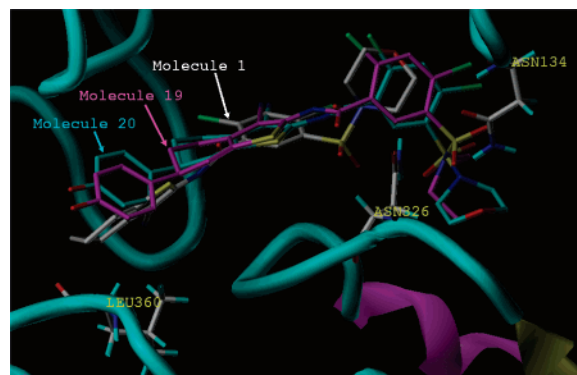

Figure 2. Molecules **1**, **19**, and **20** docked in the active site of MurF enzyme by the program GOLD.

tions of HINT score and X-CScore, the consensus score will ensure multiple sampling and avoid wrong representation of the results.[17]

An analysis of the molecular interactions of the ligands docked into the enzyme binding site reveals that the ligands are in close contact with protein residues. The cyanothiophene group in molecules **1** and **2** (Table 1) is located centrally between the N- and C-terminal domains, with the nitrile suitably oriented to form a hydrogen bond with the backbone amide of Arg49. The cycloalkyl group (cyclohexyl in molecule **1** and cyclopentyl in molecule **2**) fused to the thiophene ring extends toward a patch of hydrophobic residues from the C-terminus, making contact with the side chains of residues Pro329, Leu360, and Leu367. Phe54 interacts with the inhibitor from the N-terminal side. The chloro-substituted benzamide group and the substituted sulfonamide group are located at the interface of all three domains, resting on a hydrophobic layer formed by Phe31 and Leu45 of the N-terminal domain and Tyr135 and Ile139 of the central domain, while residues such as Asn326, Asn328, and Thr330 of the C-terminal domain are in close contact. The cyanothiophene and the amide moieties in molecules **3**, **5**, **7**, **8**, and **10** deviate from the X-ray pose of molecule **1**. A strikingly different position for molecule **12** is seen, with the cyanothiophene ring occupying the site of the morpholine group in the X-ray structure of ligands **1** and **2**: an exactly opposite (head-to-tail) orientation. This unique mode of binding might be a result of the R^3 group ($-NH-(CH_2)_3-NMe_2$) which replaces the chloro atom in molecules **1** and **2**. The most active analogs in this series, molecules **17**, **19**, and **20** have a unique phenolic substituent at R^1 and also exhibit a very different binding mode. With reference to molecule **1** or **2**, the cyanothiophene moiety in these molecules translates to occupy the position of the chlorobenzene ring in molecule **1** or **2**. This translation might take place to accommodate the *p*-hydroxyphenyl group on the cyanothiophene ring since the cavity where the cyanothiophene ring in molecule **1** binds cannot accommodate a large R^1 group. The higher activity of these three molecules stems from a major contribution of the phenolic group on the tetrahydrobenzene ring attached to the cyanothiophene ring. The phenolic OH group in molecules **17**, **19**, and **20** forms a hydrogen bond with the backbone oxygen of Leu360, whereas the sulfonamide oxygens are involved in hydrogen bonding with the amide group in the side chain of Asn134. The activity of molecule **16** may have contributions from the phenyl ring that translates the molecule in the active site
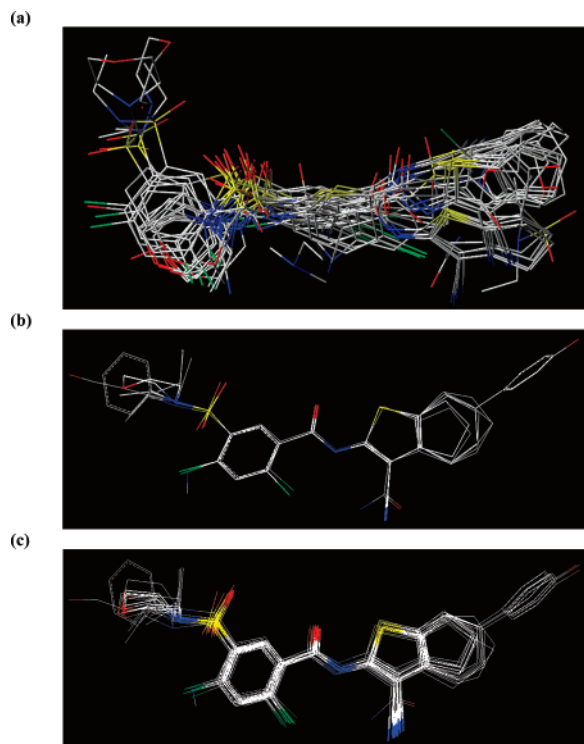
Figure 3. (a) Receptor-based, (b) atom-fit, and (c) field-fit alignments of MurF inhibitors used in the CoMFA study.

Table 2. Summary of CoMFA Models

						contributions (%)	
alignment method	N^a	r^{2b}	q^{2c}	r^2_{pred}	SEE^d	F	steric	electrostatic
receptor-based	3	0.92	0.59	0.64	0.34	50.9	41	59
atom-fit	2	0.83	0.70	0.53	0.47	35.7	75	25
field-fit	2	0.83	0.69	0.49	0.47	36.8	69	31

^{a} Optimum number of components by SAMPLS. ^{b} Conventional correlation coefficient. ^{c} Cross-validated correlation coefficient. ^{d} Standard error of estimate, training set = 18 molecules and test set = 4 molecules.

Table 3. Best CoRIA Equation and its G/PLS Statistics

CoRIA equation^a	n^b	r^{2c}	q^{2d}	LSE^e
pIC$_{50}$ = 4.48 + 0.51 (C_Thr330) − 0.53 (C_Asn134) − 9.7 (V_Lys438) − 4.96 (V_Gln363)	4	0.82	0.46	0.17

^{a} C_ and V_ in CoRIA equations indicate Coulombic and van der Waals interactions respectively. ^{b} Number of PLS components. ^{c} Conventional correlation coefficient. ^{d} Cross-validated correlation coefficient. ^{e} Least-square error, training set = 18 molecules and test set = 4 molecules.

(Figure **2**); as a result, the morpholine oxygen forms a hydrogen bond with Asn134. The amide oxygen of molecule **19** forms an additional hydrogen bond with Asn326. Molecule **20** is slightly more active than molecule **19**, which differs by having a *N,N*-diethyl substitution instead of the morpholine ring. The morpholine oxygen in molecule **20** is hydrogen bonded to the side chain amide nitrogen of Asn134 at one end, while at the other end of the molecule, the phenolic OH group hydrogen bonds to the backbone carbonyl oxygen of Leu360. This kind of (head-to-tail) stabilization of molecule **20** through hydrogen bonds may prevent easy
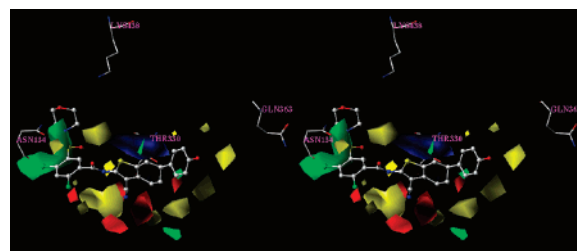

Figure 4. CoMFA contour maps for steric and electrostatic fields drawn around molecule **20** along with residues that have been found crucial to explain the variation in biological activity as revealed by the CoRIA study.
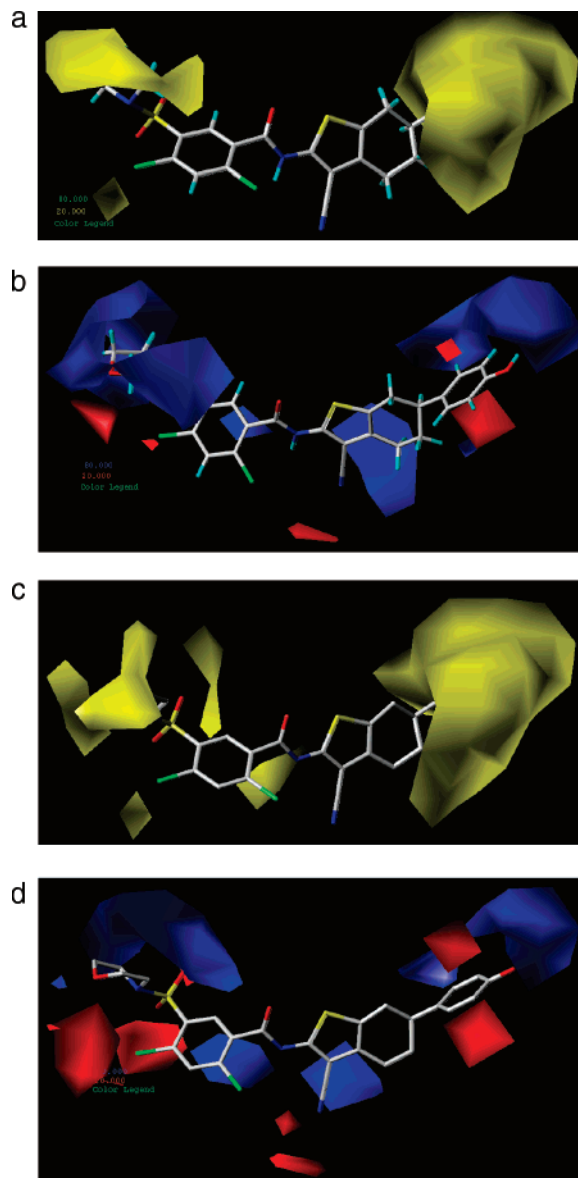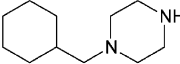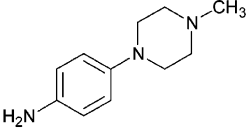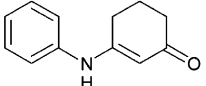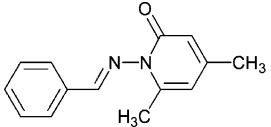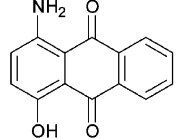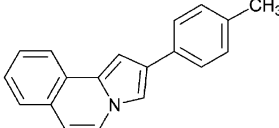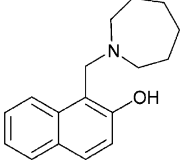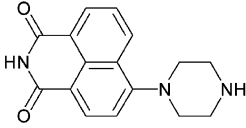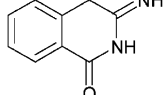

Figure 5. CoMFA contour maps for steric (a and c) and electrostatic (b and d) fields drawn around molecule **20,** derived using atom-fit (a and b) and field-fit (c and d) alignments.

diffusion of the ligand out of the enzyme binding site, leading to its higher activity. The activity difference between molecules **19** and **20** is also reflected in the HINT score which is one and half times more for **20** than for **19**; the X-CScore and GoldScore (or their constituent scores) fail to reflect this distinction of activity. These detailed interac-

Table 4. Structures of Some New Molecules Designed Using the de Novo Approach of Ludi

Mol. i.d.	Structure	pIC$_{50}$ predicted by CoRIA	pIC$_{50}$ predicted by CoMFA
1		5.5	6.2
2		5.7	6.1
3		5.2	5.5
4		5.1	4.6
5		5.0	5.5
6		5.1	5.6
7		5.7	5.9
8		5.4	5.8
9		5.2	5.6

tions of the ligands with the enzyme can be exploited in structure-based drug design.

3D-QSAR Analyses: CoMFA and CoRIA. The receptor based alignment used as input to CoMFA is shown in Figure 3, and the statistics of the CoMFA model are given in Table 2. The CoMFA models have a significant value of the square of the correlation coefficient (r^2 between 0.83 and 0.92), indicating a good correlation between the biological activity and the CoMFA descriptors, and good predictive q^2 (between 0.59 and 0.70) and r^2_{pred} values (between 0.49 and 0.64), demonstrating good internal and external predicitivity. The CoMFA steric and electrostatic contours around molecule **20** for models derived for all three alignment procedures are shown in Figures 4 and 5. The contours for the steric fields are shown in green (bulk favored) and yellow (bulk disfavored), while the electrostatic field contours are shown in red (electronegative substituents favored) and blue (electropositive substituents favored). For the CoMFA model derived using receptor-based alignment, there is a big green

contour near the morpholine ring which also encloses the sulfonamide group. There are many medium-sized yellow-colored contours around the remaining part of the molecule. Molecules with bulky substituents at the sulfonyl group that fall within the sterically favored green contours (molecules **16**, **17**, **19**, and **20**) exhibit good activity. Electrostatic features are indicated by three medium-sized red contours in the vicinity of the cyano group attached to the tetrahydrobenzothiophene ring (molecules **16**, **17**, **19**, and **20**). There is a big blue contour in a plane away from but parallel to the plane of the tetrahydrobenzothiophene ring. For the CoMFA models derived from atom-fit and field-fit alignments, big yellow steric contours appear at both substitution ends, indicating bulk being disfavored at these positions. There is no green contour at either end. The electrostatic blue and red contours as seen in Figure 4 indicate that electropositive and electronegative substitutions would be favored, respectively. The receptor-based alignment is very different from the atom-fit and field-fit alignments, which

in turn are sufficiently close to each other. The most active molecules in this series (molecules **19** and **20**) have a phenolic substitution and bind in a very different mode than the other members of the series. This mode of binding of these molecules which is different from other members of the series is a result of lack of space in the receptor active site to accommodate the bulky phenol moiety near Leu360; consequently, these molecules undergo translation in the active site (Figure **2**) which is stabilized by strong hydrogen bonding with phenolic OH. As a result, the positions and sizes of the steric and electrostatic contours associated with the CoMFA models vary appreciably between the different alignment modes.

Our recently developed 3D-QSAR approach, CoRIA[11] has been employed on the enzyme−inhibitor complexes to get hold of finer details on the factors that reflect the variation in the biological activity for these ligands. This 3D-QSAR technique uses interaction energies and specific terms describing the thermodynamics of ligand-enzyme binding as QSAR descriptors, which are correlated to the biological activity (pIC_{50}) through G/PLS statistics. One of the statistically robust CoRIA equations is listed in Table 3. The CoRIA equations indicate that Coulombic interactions with residues Thr330 and Asn134 are important for amending the activity; this is also seen with the CoMFA contours occupying the side chain of Thr330 when the CoMFA model is superimposed onto the active site of the enzyme. In addition, the van der Waals interactions with residues Lys438 and Gln363 are indicated to be important for modulating the biological activity. Analysis of the ten best equations reveals that van der Waals interactions with additional residues such as Ile335, Gln363, Ser364, and Gly47 should also be considered for regulating the activity. The most potent inhibitor, molecule **20,** surrounded by residues revealed by CoRIA as important for modifying activity are shown in Figure 4. Thus, according to CoRIA results, optimization the Coulombic interaction of ligands with the above-mentioned residues will stabilize binding and improve their potency.

De Novo Design of MurF Inhibitors. It is heartening to note that the inhibitors designed using Ludi are seen to interact with the same active site residues which have been revealed in the docking and CoRIA studies. The affinities of the molecules designed through Ludi have been predicted with the CoMFA model derived using receptor-based alignment and the CoRIA model (Table 3). The structures of some novel inhibitors derived by this approach and their activities as predicted by the CoMFA and CoRIA models have been summarized in Table 4. The designed molecules bear the properties of lead-like molecules (rule-of-three)[25] such as MW below 300, number of H-bond donors/acceptors less than 3, and log *P* less than 3, so that after lead optimization, the drug-like molecules will fulfill Lipinski's rule-of-five.[26] These moieties offer a basic lead for recognition by the MurF active site and can be further optimized for potency.

CONCLUSIONS

The search for new antibacterial agents directed toward novel targets has become highly imperative as a result of the recent emergence of cross-resistance by almost all pathological microorganisms. Since the mid-1990s, inhibitors of the Mur cytoplasmic enzymes had begun to appear, and

more recently these enzymes have attained a great deal of attention as a target for the development of antibacterial therapy. The present study is an attempt at a thorough and systematic understanding of MurF−inhibitor interactions at the molecular level using a variety of structure-based modeling approaches. Successful docking and scoring protocols have been established for this class of ligands and its associated enzyme. A good correlation of the biological activity with HINT score and X-CScore has been observed. 3D-QSAR models have been developed using the receptor-based alignment of the docked ligands using CoMFA, as well as from the information of ligand−receptor interactions at the residue level through CoRIA. The QSAR models were used to predict the activities of molecules designed using the de novo approach of Ludi. This study provides valuable results in the search and rational design of new generation of specific bacterial cell wall inhibitors.

REFERENCES AND NOTES

(1) (a) Davies, J. Inactivation of antibiotics and the dissemination of resistance genes. *Science* **1994**, *264*, 375−382. (b) Cohen, M. L. Epidemiology of drug resistance: Implications for a post-antimicrobial era. *Science* **1992**, *257*, 1050−1055. (c) Neu, H. C. The crisis in antibiotic resistance. *Science* **1992**, *257*, 1064−1073.

(2) Gale, E. F.; Cundliffe, E.; Reynolds, P. E.; Richmond, M. H.; Waring, M. J. In *The Molecular Basis of Antibiotic Action*, 2nd ed.; Wiley and Sons: London, 1981.

(3) van Heijenoort, J. In *Escherichia coli and Salmonella*; Neidhardt, F. C., Curtis, R., III, Ingraham, J. L., Lin, E. C. C., Low, K. B., Magasanik, B., Resnikoff, W. S., Riley, M., Schaechter, M., Umbarger, H. E., Eds.; American Society for Microbiology: Washington, DC, 1996; pp 1025−1034.

(4) Anderson, M. S.; Eveland, S. S.; Onishi, H. R.; Pompliano, D. L. Kinetic mechanism of the *Escherichia coli* UDPMurNAc-tripeptide. D-alanyl-D-alanine-adding enzyme: Use of a glutathione *S*-transferase fusion. *Biochemistry* **1996**, *35*, 16264−16269.

(5) Zoeiby, A. E.; Sanschagrin, F.; Levesque, R. C. Structure and function of the Mur enzymes: Development of novel inhibitors. *Mol. Microbiol.* **2003**, *47*, 1−12.

(6) Miller, D. J.; Hammond, S. M.; Anderluzzi, D.; Bugg, T. D. Aminoalkylphosphinate inhibitors of D-Ala-D-Ala adding enzyme. *J. Chem. Soc., Perkin Trans 1* **1998**, *1*, 131−142.

(7) Gu, Y. G.; Florjancic, A. S.; Clark, R. F.; Zhang, T.; Cooper, C. S.; Anderson, D. D.; Lerner, C. G.; McCall, J. O.; Cai, Y.; Black-Schaefer, C. L.; Stamper, G. F.; Hajduk, P. J.; Beutel, B. A. Structure−activity relationships of novel potent MurF inhibitors. *Bioorg. Med. Chem. Lett.* **2004**, *14*, 267−270.

(8) Berman, H. M.; Westbrook, J.; Feng, Z.; Gilliland, G.; Bhat, T. N.; Weissig, H.; Shindyalov, I. N.; Bourne, P. E. The Protein Data Bank. *Nucleic Acids Res.* **2000**, *28*, 235−242.

(9) Longenecker, K. L.; Stamper, G. F.; Hajduk, P. J.; Fry, E. H.; Jakob, C. G.; Harlan, J. E.; Edalji, R.; Bartley, D. M.; Walter, K. A.; Solomon, L. R.; Holzman, T. F.; Gu, Y. G.; Lerner, C. G.; Beutel, B. A.; Stoll, V. S. Structure of MurF from *Streptococcus pneumoniae* co-crystallized with a small molecule inhibitor exhibits interdomain closure. *Protein Sci.* **2005**, *14*, 3039−3047.

(10) Cramer, R. D.; Patterson, D. E.; Bunce, J. D. Comparative molecular field analysis (CoMFA). 1. Effect of shape on binding of steroids to carrier proteins. *J. Am. Chem. Soc.* **1988**, *110*, 5959−5967.

(11) Datar, P. A.; Khedkar, S. A.; Malde, A. K.; Coutinho, E. C. Comparative residue interaction analysis (CoRIA): A 3D-QSAR

approach to explore the binding contributions of active site residues with ligands. *J. Comput.-Aided Mol. Des.* **2006**, *20*, 343−360.

(12) Halgren, T. Maximally diagonal force constants in dependent angle-bending coordinates. II. Implications for the design of empirical force fields. *J. Am. Chem. Soc.* **1990**, *112*, 4710−4723.

(13) (a) Jones, G.; Willett, P.; Glen, R. C.; Leach, A. R.; Taylor, R. Development and validation of a genetic algorithm for flexible docking. *J. Mol. Biol.* **1997**, *267*, 727−748. (b) Jones, G.; Willett, P.; Glen, R. C. Molecular recognition of receptor sites using a genetic algorithm with a description of desolvation. *J. Mol. Biol.* **1995**, *245*, 43−53. (c) Jones, G.; Willett, P.; Glen, R. C. A genetic algorithm for flexible molecular overlay and pharmacophore elucidation. *J. Comput.-Aided Mol. Des.* **1995**, *9*, 532−549.

(14) *GOLD*, version 3.1; Cambridge Crystallographic Data Centre: Cambridge, U.K., 2006.

(15) (a) Eldridge, M. D.; Murray, C. W.; Auton, T. R.; Paolini, G. V.; Mee, R. P. Empirical scoring functions: I. The development of a fast empirical scoring function to estimate the binding affinity of ligands in receptor complexes. *J. Comput.-Aided Mol. Des.* **1997**, *11*, 425−445. (b) Baxter, C. A.; Murray, C. W.; Clark, D. E.; Westhead, D. R.; Eldridge, M. D. Flexible docking using Tabu search and an empirical estimate of binding affinity. *Proteins* **1998**, *33*, 367−382.

(16) (a) Kellogg, G. E.; Semus, S. F.; Abraham, D. J. *HINT*: A new method of empirical hydrophobic field calculation for CoMFA. *J. Comput.-Aided Mol. Des.* **1991**, *5*, 545−552. (b) Kellogg, G. E.; Joshi, G. S.; Abraham, D. J. New tools for modeling and understanding hydrophobicity and hydrophobic interactions. *Med. Chem. Res.* **1992**, *36*, 444−453. (c) *Sybyl HINT*; Tripos Inc: St. Louis, MO, 2005.

(17) Wang, R.; Lai, L.; Wang, S. Further development and validation of empirical scoring functions for structure-based binding affinity prediction. *J. Comput.-Aided Mol. Des.* **2002**, *16*, 11−26.

(18) Wang, R.; Gao, Y.; Lai, L. SCORE: A New Empirical Method for Estimating the Binding Affinity of a Protein-Ligand Complex *J. Mol. Model.* **1998**, *4*, 379−394.

(19) (a) Böhm, H. J. A novel computational tool for automated structure-based drug design. *J. Mol. Recognit.* **1993**, *6*, 131−137. (b) Böhm, H. J. The computer program LUDI: A new method for the de novo design of enzyme inhibitors. *J. Comput.-Aided Mol. Des.* **1992**, *6*, 61−78. (c) Böhm, H. J. LUDI: Rule based automatic design of new substituents for enzyme inhibitor leads. *J. Comput.-Aided Mol. Des.* **1992**, *6*, 593−606. (d) Böhm, H. J. The development of a simple empirical scoring function to estimate the binding constant for a protein−ligand complex of known three-dimensional structure. *J. Comput.-Aided Mol. Des.* **1994**, *8*, 243−256. (e) Böhm, H. J. On the use of LUDI to search the Fine Chemicals Directory for ligands of proteins of known three-dimensional structure. *J. Comput.-Aided Mol.*

Des. **1994**, *8*, 623−632. (f) Stahl, M.; Böhm, H. J. Development of filter functions for protein−ligand docking. *J. Mol. Graph. Model.* **1998**, *16*, 121−132. (g) Böhm, H. J. Prediction of binding constants of protein ligands: a fast method for the prioritization of hits obtained from de novo design or 3D database search programs. *J Comput.-Aided Mol. Des.* **1998**, *12*, 309−323.

(20) (a) Vedani, A.; Dobler, M. 5D-QSAR: The key for simulating induced fit? *J. Med. Chem.* **2002**, *45*, 2139−2149. (b) Vedani, A.; Dobler, M.; Lill, L. Combining protein modeling and 6D-QSAR−Simulating the binding of structurally diverse ligands to the estrogen receptor. *J. Med. Chem.* **2005**, *48*, 3700−3703.

(21) (a) Rogers, D.; Hopfinger, A. J. *J. Chem. Inf. Comput. Sci.* **1994**, *34*, 854−866. (b) Kubinyi, H., Ed. *3D QSAR in Drug Design: Theory, Methods and Applications*; ESCOM, Leiden, The Netherlands, 1993; pp. 523−550.

(22) Ikeda, M.; Wachi, M.; Jung, H. K.; Ishino, F.; Matsuhashi, M. Nucleotide sequence involving MurG and MurC in the mra gene cluster region of *Escherichia coli*. *Nucleic Acids Res.* **1990**, *18*, 4014.

(23) (a) Yan, Y.; Munshi, S.; Li, Y.; Pryor, K. A.; Marsilio, F.; Leiting, B. Crystallization and preliminary X-ray analysis of the *Escherichia coli* UDP-MurNAc-tripeptide D-alanyl−D-alanine-adding enzyme (MurF). *Acta. Crystallogr., Sect. D :Biol. Crystallogr.* **1999**, *55*, 2033−2034. (b) Yan, Y.; Munshi, S.; Leiting, B.; Anderson, M. S.; Chrzas, J.; Chen, Z. Crystal structure of Escherichia coli UDP-MurNAc-tripeptide D-alanyl−D-alanine-adding enzyme (MurF) at 2.3 Å resolution. *J. Mol. Biol.* **2000**, *304*, 435−445.

(24) (a) Baber, J. C.; Shirley, W. A.; Gao, Y.; Feher, M. The use of consensus scoring in ligand-based virtual screening. *J. Chem. Inf. Model.* **2006**, *46*, 277−288. (b) Oda, A.; Tsuchida, K.; Takakura, T.; Yamaotsu, N.; Hirona, S. Comparison of consensus scoring strategies for evaluation computational models of protein-ligand complexes, *J. Chem. Inf. Model.* **2006**, *46*, 380−391. (c) Muegge, I.; Rarey, M. Small molecule docking and scoring. *Rev. Comput. Chem.* **2001**, *17*, 1−60.

(25) Congreve, M.; Carr, R.; Murray, C.; Jhoti, H. A A "Rule of three" for fragment-based lead discovery? *Drug Discovery Today* **2003**, *8*, 876−877.

(26) (a) Lipinski, C. A.; Lombardo, F.; Dominy, B. W.; Feeney, P. J. Experimental and computational approaches to estimate solubility and permeability in drug discovery and development settings. *Adv. Drug Delivery Rev.* **1997**, *23*, 3−25. (b) Lipinski, C. A.; Lombardo, F.; Dominy, B. W.; Feeney, P. J. Experimental and computational approaches to estimate solubility and permeability in drug discovery and development settings, *Adv. Drug Delivery Rev.* **2001**, *46*, 3−26.